Minimal leptogenesis in brane-inspired cosmology

Alessandro Di Marco,[1,*] Amit Dutta Banik,[2,†] Anish Ghoshal,[3,‡] and Gianfranco Pradisi[4,§]

[1]*Istituto Nazionale di Astrofisica, Istituto di Astrofisica e Planetologia Spaziali (INAF-IAPS), Via Fosso del Cavaliere, 100, 00133 Rome, Italy*

[2]*Physics and Applied Mathematics Unit, Indian Statistical Institute, Kolkata-700108, India*

[3]*Institute of Theoretical Physics, Faculty of Physics, University of Warsaw, ul. Pasteura 5, 02-093 Warsaw, Poland*

[4]*University of Rome "Tor Vergata" and INFN, Sezione di Roma "Tor Vergata", via della Ricerca Scientifica 1, 00133 Roma, Italy*

(Received 29 November 2022; accepted 25 March 2023; published 10 May 2023)

We discuss how a post-inflationary reheating phase characterized by a nonstandard multiple scalar field cosmology can change the thermal history of the Universe, affecting minimal high-scale leptogenesis. In particular, we explore a class of models where a set of scalar fields in a brane-inspired dynamical scenario modifies the Boltzmann equations concerning standard leptogenesis. The produced lepton asymmetry Y_L, due to the decays of heavy Majorana right-handed neutrinos responsible for generating Standard Model neutrino masses via the type-I seesaw, is affected as well. In particular, both an enhancement and a reduction of Y_L can be obtained, depending on the values of the (new) involved parameters and on the number of additional scalar fields.

DOI: 10.1103/PhysRevD.107.103509

I. INTRODUCTION

The theory of cosmological inflation [1] represents an awesome solution to the long-standing conundrums affecting the standard cosmology, i.e., the flatness problem, the horizon problem, and the monopole problem. Inflation also provides a natural explanation for the seeds, namely, the primordial scalar metric fluctuations generating the matter inhomogeneities, responsible for both the growth of the large-scale structures visible in the Universe and the temperature anisotropies of the cosmic microwave background. Moreover, primordial gravitational waves are naturally produced during the accelerated expansion and their detection—which is possible if the involved energy scale is high enough—would represent a remarkable smoking gun for inflation. In its simplest version—the so-called single-field slow-roll inflation—the inflationary mechanism is driven by a homogeneous, neutral, and minimally coupled scalar field ϕ, called the inflation field, typically characterized by an effective scalar potential $V(\phi)$ equipped with an (almost) flat region and a fundamental vacuum state. In the first stage of inflation, the scalar field slowly crosses the plateau of the scalar potential, which behaves like a cosmological constant and triggers an (almost) de Sitter expansion of the Universe. At the end of the inflationary period, the inflaton field reaches the steep region of the potential and falls into the global vacuum where it starts to oscillate. As a consequence, it should then decay to Standard Model (SM) and beyond-the-SM (BSM) relativistic particles, reheating the cold Universe and giving rise to the graceful exit toward the standard initial radiation-dominated hot big bang (HBB) epoch (for reviews on reheating, see Ref. [2]). Of course, the simplest mentioned scenario is not mandatory. The Universe could have experienced nonstandard post-reheating and pre–big bang nucleosynthesis (BBN) cosmological phases driven by one or more additional scalar fields, recovering the radiation dominance at lower energy scales. An intriguing possibility, first noticed in Ref. [3], is represented by the presence of additional sterile scalar fields characterized by a faster-than-radiation scaling law of the corresponding energy density. As new cosmological components, they can provide interesting modifications of the dark matter annihilation rates and relics [3–7], inflationary e-folds [8,9], lepton and baryon asymmetry generation [10,11], matter–dark matter cogenesis [12], and gravitational-wave signals [13].

These scalars are common in theories with extra dimensions and branes [14], like superstring orientifold models [15]. Indeed, scalars parametrizing the positions of

*alessandro.dimarco1@inaf.it
†amitdbanik@gmail.com
‡anish.ghoshal@fuw.edu.pl
§gianfranco.pradisi@roma2.infn.it

D-branes along the transverse internal directions interact gravitationally with the metric sector and can be engineered in a way to be decoupled by the longitudinal oscillation modes, related to SM and BSM fields. In this paper, we consider nonstandard cosmologies inspired by orientifolds with D-branes containing, generically, multiple sterile scalar fields entering a nonstandard post-reheating phase. We study their effects on minimal thermal leptogenesis, extending the analysis of Ref. [10], where the single-field case was addressed.

The term leptogenesis refers to the process of generation of lepton asymmetry and (induced) baryon asymmetry in the Universe. The simplest class of models employs the decay of heavy right-handed neutrinos (RHNs) in the type-I seesaw mechanism [16]. The process involves CP-violating, out-of-equilibrium decay of lepton-number-violating RHNs. There are also a number of versions of leptogenesis depending on, for instance, the choice of seesaw mechanism (type II or type III) or the presence of supersymmetry (soft leptogenesis) [17], or even ones using radiative generation [18]. Complete reviews on leptogenesis can be found in Ref. [19].

We limit ourselves to the analysis of the effects of the mentioned insertion of multiple scalar fields on the minimal type-I seesaw leptogenesis, although we expect that similar modifications could be applied to other leptogenesis scenarios as well.

The paper is organized as follows. In Sec. II we briefly discuss nonstandard cosmology in the post-reheating early-Universe epoch, with the presence of scalar fields inspired by properties of (super)string theory vacua. In Sec. III we discuss how standard thermal leptogenesis is modified by the presence of a number of k scalar fields, and discuss the two-scalar-field case in detail. In Sec. IV we repeat the study of nonstandard leptogenesis in the presence of three active scalar fields. Finally, in Sec. V we summarize our obtained results and discuss some open problems. In this paper we use the particle natural units $\hbar = c = 1$, and $M_P = 1/\sqrt{8\pi G_N}$ is the reduced Planck mass, where G_N is the gravitational Newton's constant.

II. D-BRANE SCALARS AND NONSTANDARD COSMOLOGY

In the standard HBB scenario, after reheating the Universe should experience a very hot and dense radiation-dominated era. In that phase, the evolution of the Universe is well described by a homogeneous fluid that obeys the Friedmann equation

$$H^2(T) \simeq \frac{1}{3M_P^2}\rho_{\rm rad}(T), \tag{1}$$

where the radiation energy density at temperature T is

$$\rho_{\rm rad}(T) = \frac{\pi^2}{30} g_E(T) T^4, \tag{2}$$

where $H = \dot{a}/a$ denotes the Hubble rate in a Friedmann-Lemaître-Robertson-Walker metric whose $a(t)$ is the standard cosmic scale factor, while g_E is the effective number of relativistic degrees of freedom, which turns out to be

$$g_E(T) = \sum_b g_b \left(\frac{T_b}{T}\right)^4 + \frac{7}{8}\sum_f g_f \left(\frac{T_f}{T}\right)^4, \tag{3}$$

where b and f label bosonic and fermionic contributions, respectively, while T_b and T_f indicate the corresponding temperatures. However, since the reheating phase is largely unknown, there is room for many scenarios involving a graceful exit from inflation and a corresponding modified path to the HBB era of a radiation-dominated universe. A simple possibility consists in a cosmological stress-energy tensor that, after reheating, could be dominated by non-interacting scalar fields equipped with a faster-than-radiation dilution law of the corresponding energy density. These kind of components are quite common in both scalar modifications of general relativity and theories with extra dimensions. Among them, (super)string theories are (the only) consistent proposals for a UV quantum completion of general relativity. Moreover, many scalars are naturally present in their spectra. In four dimensions, the scalars result from dimensional reduction of ten-dimensional fields and parametrize the deformations of the internal (compact) manifolds. In orientifold models, which are genuine string theory vacua, additional scalar fields are related to the presence of D-branes, namely of topological defects where openstring ends can slide. Indeed, the position of space-time-filling branes along the internal directions are additional parameters that correspond to scalar fields in the effective low-energy action. At tree level, the scalars are moduli, i.e., their potential vanishes and their interactions are purely gravitational. In order to stabilize most of them, a known procedure is to introduce flux compactifications, namely, by adding vacuum expectation values to some of the internal (form) fields in the spectra. This way, one also gets (partial spontaneous) breaking of supersymmetry and backreaction on the space-time geometry, resulting into a warping of the metric. The generated scalar potentials are typically steep or dominated by kinetic terms, making the corresponding fields possibly active after the reheating phase. In particular, we consider a set of scalar fields that only interact with the inflaton but are are completely decoupled from the remaining degrees of freedom. They correspond to positions in the transverse internal directions of a number of well-separated[1] D-branes whose dynamics is decoupled from the visible sector (i.e., the SM fields), other possible hidden (dark) matter sectors, and even the fields related to the longitudinal degrees of freedom on the

[1]We assume that the branes move slowly in the compact space, while the potential felt by their position gives rise to a quick dilution due to the exotic nature of the corresponding fluid.

brane itself. Their mutual interactions can also be neglected and the position fluctuations do not interfere with each other. One example of this kind of scenario was given in Refs. [8,14], where the transverse position of a probe D-brane behaved exactly as requested once the Dirac-Born-Infeld and Wess-Zumino terms describing its dynamics were specialized to a warped geometry. In this sense, we consider them as "brane-inspired" models (for a review on some aspects of string cosmology with branes, see, e.g., Ref. [20]). Obviously, a similar number of scalars can also be introduced by hand without any reference to brane configurations. As said, the most important point is that these scalar fields always interact with the inflaton, which can thus decay to them and to the remaining (relativistic) components of the standard reheating fluid. The previous conditions are necessary in order to avoid relics moduli fields that overclose the Universe or ruin BBN. Let us thus analyze a modification of the evolution of the early Universe after the reheating phase, realized through the presence of the mentioned set of scalar fields $\phi_i (i = 1, \dots, k)$ [9]. They are assumed to dominate at different time scales until radiation becomes the most relevant component, well before the BBN era in order to guarantee the predictions about the light element abundances. Given the assumptions, the total energy density after the inflaton decay can be assumed to be

$$\rho_{\rm tot}(T) = \rho_{\rm rad}(T) + \sum_{i=1}^{k} \rho_{\phi_i}(T). \tag{4}$$

We introduce the scalar fields in such a way that, for $i > j$, ρ_{ϕ_i} hierarchically dominates at higher temperatures over ρ_{ϕ_j} when the temperature decreases. All of the scalar fields, which are supposed to be completely decoupled from each other and from matter and radiation fields, can be described as perfect fluids diluting faster than radiation. In this respect, the dynamics is encoded in

$$\dot{\rho}_{\phi_i} + 3H\rho_{\phi_i}(1 + w_i) = 0, \tag{5}$$

where $w_i = w_{\phi_i}$ is the equation-of-state parameter of the field ϕ_i. Integrating this equation, one finds

$$\rho_{\phi_i}(T) = \rho_{\phi_i}(T_i)\left(\frac{a(T_i)}{a(T)}\right)^{4+n_i}, \tag{6}$$

with $n_i = 3w_i - 1$. The indices[2] n_i, namely, the "dilution" coefficients, satisfy the conditions

$$n_i > 0, \qquad n_i < n_{i+1}. \tag{7}$$

T_i can be conveniently identified with the transition temperature at which the contribution of the energy density of ϕ_i becomes subdominant with respect to that of ϕ_{i-1}. In other words, the scalar fields are such that

$$\rho_{\phi_i} > \rho_{\phi_{i-1}} \quad \text{for } T > T_i, \tag{8}$$

$$\rho_{\phi_i} = \rho_{\phi_{i-1}} \quad \text{for } T = T_i, \tag{9}$$

$$\rho_{\phi_i} < \rho_{\phi_{i-1}} \quad \text{for } T < T_i. \tag{10}$$

By using the conservation of the "comoving" entropy density

$$g_S(T)a^3(T)T^3 = g_S(T_i)a^3(T_i)T_i^3, \tag{11}$$

where the effective number of relativistic degrees of freedom associated with entropy g_S is defined by

$$g_S(T) = \sum_b g_b\left(\frac{T_b}{T}\right)^3 + \frac{7}{8}\sum_f g_f\left(\frac{T_f}{T}\right)^3, \tag{12}$$

the energy density of the various fields at a temperature T can be expressed in terms of the transition temperatures T_i as

$$\rho_{\phi_i}(T) = \rho_{\phi_i}(T_i)\left(\frac{g_S(T)}{g_S(T_i)}\right)^{\frac{4+n_i}{3}}\left(\frac{T}{T_i}\right)^{4+n_i}. \tag{13}$$

For the first scalar field ϕ_1, by definition, the transition temperature coincides with that at the beginning of the radiation-dominated era, $T_1 = T_r$, so that $\rho_{\phi_1}(T_1) = \rho_{\rm rad}(T_1)$. The second scalar field ϕ_2 is subdominant compared to ϕ_1 below the temperature T_2. Using Eq. (13) and observing that T_2 is the transition temperature at which $\rho_{\phi_2}(T_2) = \rho_{\phi_1}(T_2)$, one gets

$$\rho_{\phi_2}(T) = \rho_{\phi_1}(T_1)\left(\frac{T_2 g_S^{1/3}(T_2)}{T_1 g_S^{1/3}(T_1)}\right)^{4+n_1}\left(\frac{T g_S^{1/3}(T)}{T_2 g_S^{1/3}(T_2)}\right)^{4+n_2}. \tag{14}$$

This equation tells us that the energy density of the scalar field ϕ_2 depends on the ratio between the two scales T_1 and T_2, where the ϕ_1 dominance occurs. In the same way, we can derive the analogous expressions for the other scalar fields. The energy density carried by the ith field ϕ_i can thus be written as

$$\rho_{\phi_i}(T) = \rho_{\rm rad}(T_r)\prod_{j=1}^{i-1}\left(\frac{T_{j+1} g_S^{1/3}(T_{j+1})}{T_j g_S^{1/3}(T_j)}\right)^{4+n_j} \times \left(\frac{T g_S^{1/3}(T)}{T_i g_S^{1/3}(T_i)}\right)^{4+n_i}, \quad i \geq 2, \tag{15}$$

[2] It should be noticed that the n_i's are not necessarily integers, even though in this paper, for simplicity, we assign them integer values. Moreover, the scalar fields with $n_i > 2$ represent ultrastiff fluids with a (dynamically generated) $w > 1$. These are perfectly consistent components, as shown in detail and with examples in Ref. [3] and references therein. They dilute quite rapidly and consequently are able to dominate the Universe only at very primordial stages. They can also play an important role in "oscillating universes" like, for example, the ekpyrotic scenario; see Ref. [21].

and, inserted into Eq. (4), this allows to calculate the total energy density dominating the expansion of the Universe after the standard reheating phase, up to the beginning of the radiation-dominated epoch. In particular, using Eq. (2), one has[3]

$$\rho(T) = \rho_{\rm rad}(T)\mathcal{J}^2(T), \tag{16}$$

where the (positive) "correction factor" determining the nonstandard evolution in the presence of k additional scalar fields is

$$\mathcal{J}^2(T) = 1 + \left(\frac{T_r g_E^{1/4}(T_r)}{T g_E^{1/4}(T)}\right)^4 \left(\frac{T g_S^{1/3}(T)}{T_1 g_S^{1/3}(T_1)}\right)^{4+n_1} + \sum_{i=1}^{k} \left(\frac{T_r g_E^{1/4}(T_r)}{T g_E^{1/4}(T)}\right)^4 \left(\frac{T g_S^{1/3}(T)}{T_i g_S^{1/3}(T_i)}\right)^{4+n_i} \times \prod_{j=1}^{i-1} \left(\frac{T_{j+1} g_S^{1/3}(T_{j+1})}{T_j g_S^{1/3}(T_j)}\right)^{4+n_j}. \tag{17}$$

Since, by assumption, there is no change in the number of degrees of freedom between the end of the reheating phase and the beginning of the HBB phase, all of the ratios of g_S and g_E at different temperatures are of order 1. Thus, for sufficiently high T and k additional scalar fields, it turns out that (defining $n_0 = 0$)

$$\mathcal{J}^2(T) \simeq 1 + \sum_{i=1}^{k} \prod_{j=1}^{i} \left(\frac{T}{T_j}\right)^{n_j - n_{j-1}}. \tag{18}$$

As expected, the larger the number of additional scalar fields, the larger the correction factor. Typically, in string-inspired models one cannot have $k \to \infty$ because the number of scalar fields is related to the number of branes and the geometric deformations of the internal compactification manifold, which are both limited by the rank of the gauge group and the number of extra dimensions, respectively.[4] Moreover, it is important to underline a couple of fundamental aspects. First, the properties of these scalars (i.e., dilution parameters and transition temperatures) cannot be completely arbitrary. In particular, it should be guaranteed that the energy density at the production scale (the reheating epoch) should not be larger than some cutoff M, bounded by the inflationary scale $M_{\rm inf}$. As a consequence, a corresponding strong bound on the reheating temperature $T_{\rm reh}$ is demanded [9]. For instance, in the case of a single nonstandard post-reheating scalar with a dilution parameter n_1 and a transition-to-radiation temperature $T_1 = T_r$, the necessary condition is just $\rho_{\phi_1}(T_{\rm reh}) \le M^4$, which leads to the bound

$$T_{\rm reh} \le \alpha_1 M \left(\frac{T_1}{M}\right)^{\frac{n_1}{4+n_1}}, \qquad \alpha_1 = \left(\frac{30}{\pi^2 g_E}\right)^{\frac{1}{4+n_1}}. \tag{19}$$

In the case of a pair of nonstandard post-reheating scalars, with ϕ_2 dominating the Universe for $T > T_2$ and being superseeded by ϕ_1 for $T < T_2$, the necessary condition becomes $\rho_{\phi_2}(T_{\rm reh}) \le M^4$ at $T = T_{\rm reh}$. As a consequence, one gets

$$T_{\rm reh} \le \alpha_2 M \left(\frac{T_1^{n_1} T_2^{n_2 - n_1}}{M^{n_2}}\right)^{\frac{1}{4+n_2}}, \qquad \alpha_2 = (30/\pi^2 g_E)^{1/4+n_2}, \tag{20}$$

where, by assumption, $n_2 > n_1$. Of course, similar expressions can be easily found for more than two additional scalar fields. The second point we would like to stress is that the presence of these additional early cosmological phases typically alters the inflationary number of e-folds [8,9] with an extra contribution $\Delta N(\phi_i, T_{\rm reh})$ proportional to the (logarithm of) $\mathcal{J}(T_{\rm reh})$, i.e.,

$$N_* \sim \xi_* - \frac{1 - 3w_{\rm reh}}{3(1 + w_{\rm reh})} \ln\left(\frac{M_{\rm inf}}{T_{\rm reh}}\right) + \ln\left(\frac{M_{\rm inf}}{M_{\rm Pl}}\right) + \frac{2}{3(1 + w_{\rm reh})} \ln \mathcal{J}(T_{\rm reh}), \tag{21}$$

where $\xi_* \sim 64$ and $w_{\rm reh}$ is the mean value of the equation-of-state parameter of the reheating fluid. Thereby, this extra factor depends on the additional setup of scalar fields (namely, the number of scalars and dilution indices) and the properties of the reheating scale. However, reasonable assumptions provide an *enhancement* of the number of e-folds of the order of 5–15, also allowing refined predictions for most of the inflationary models. The details of the modification of the tensor-to-scalar ratio r or on tensor power spectra $P_T(k)$ induced by these nonstandard cosmologies were broadly discussed in Refs. [9,13].

III. NONSTANDARD HISTORY OF LEPTOGENESIS WITH TWO SCALAR FIELDS

In this section we probe the effects on leptogenesis of the described fast expansion of the Universe with multiple scalar fields. We consider the simple type-I seesaw mechanism including heavy Majorana RHNs that generate a lightest neutrino and induce lepton number violation. Complex Yukawa interactions with leptons result in CP violation when the RHN decay processes are considered with loop-mediated interactions. Finally, the out-of-equilibrium decay of RHNs (or of the lightest RHN N_1, the so-called N_1 leptogenesis that we use here) produces the baryon

[3]It should be noticed that the amplification parameter $\mathcal{J}^2(T)$ is the $\eta(T)$ parameter of Ref. [9].

[4]Typically, "before" moduli stabilization, one has $\mathcal{O}(100)$ moduli from the compactification manifold and a net number of $\mathcal{O}(30)$ branes. Of course, the number of brane moduli can be made arbitrarily large by including brane-antibrane pairs.

asymmetry of the Universe. The relevant portion of the lagrangian density describing this process is given (for three generations) by

$$\mathcal{L}_{\rm RHN} = -\lambda_{ik}\bar{l}_i N_k - \frac{1}{2}M_k \overline{N}^c{}_k N_k + \text{H.c.}, \quad i,k = 1,2,3, \tag{22}$$

where a diagonal flavor basis is selected for the RHNs. The SM Higgs doublet is denoted by Φ, the corresponding conjugate is $\tilde{\Phi}$, and l indicates an SM lepton doublet. With the above BSM extension, one obtains an active neutrino mass matrix,

$$M_\nu = -m_D^T M^{-1} m_D, \tag{23}$$

where m_D denotes the Dirac mass matrix with entries of order $\mathcal{O} \sim v_\Phi \lambda$ (v_Φ is the vacuum expectation value of the Higgs doublet) and M is the diagonal RHN mass matrix. As mentioned, the amount of CP asymmetry generated in the process of N_1 decay for a hierarchical RHN mass distribution $M_3, M_2 \gg M_1$ is measured by

$$\epsilon = \frac{\sum_\alpha [\Gamma(N_1 \to l_\alpha + \Phi) - \Gamma(N_1 \to \bar{l}_\alpha + \Phi^*)]}{\Gamma_1} = -\frac{3}{16\pi}\frac{1}{(\lambda^\dagger\lambda)_{11}}\sum_{k=2,3}\text{Im}[(\lambda^\dagger\lambda)^2_{1j}]\frac{M_1}{M_k}, \tag{24}$$

with $\Gamma_1 = \frac{M_1}{8\pi}(\lambda^\dagger\lambda)_{11}$ being the total decay width of the lightest RHN N_1. The asymmetry parameter ϵ can be used to provide a limit on the N_1 mass via the Casas-Ibarra parametrization formalism [22]. Indeed, it turns out that

$$|\epsilon| \le \frac{3}{16\pi v_\Phi^2} M_1 m_\nu^{\max}, \tag{25}$$

with $m_\nu^{\max}$ being the largest light neutrino mass. As a consequence, a lower bound (the Davidson-Ibarra bound [23], $M_1 \gtrsim 10^9$ GeV) emerges for the M_1 mass of the lightest RHN, when neutrino oscillation parameters are taken into account. N_1 leptogenesis, effective at temperatures $T \gtrsim 10^{12}$ GeV, also induces a constraint on the reheating temperature after inflation at values $T_{\rm reh} > 10^{12}$ GeV. Disregarding the possibility of flavored leptogenesis, we limit ourselves to the usual thermal leptogenesis, solving for the simplified Boltzmann equations (BEs). In standard cosmology with a radiation-dominated Universe after reheating, they can be written as

$$\frac{dY_{N_1}}{dz} = -z\frac{\Gamma_1}{H_1}\frac{\mathcal{K}_1(z)}{\mathcal{K}_2(z)}(Y_{N_1} - Y_{N_1}^{EQ}), \tag{26}$$

$$\frac{dY_L}{dz} = -\frac{\Gamma_1}{H_1}\left(\epsilon z\frac{\mathcal{K}_1(z)}{\mathcal{K}_2(z)}(Y_{N_1}^{EQ} - Y_{N_1}) + \frac{z^3\mathcal{K}_1(z)}{4}Y_L\right). \tag{27}$$

In Eqs. (26)–(27), $Y_i = n_i/s$ denotes the abundance of the particle i, namely, the ratio of its number density to the entropy density, while $Y_L = (Y_l - Y_{\bar{l}})$ is the lepton asymmetry. The equilibrium abundance of the lightest RHN is [19,24]

$$Y_{N_1}^{EQ} = \frac{45g}{4\pi^4}\frac{z^2\mathcal{K}_2(z)}{g_S}. \tag{28}$$

It should be noticed that Eqs. (26)–(27) both depend on the modified Bessel functions ($\mathcal{K}_{1,2}$), the Hubble parameter $H_1 = H(T = M_1) = H(T)z^2$, and the decay width Γ_1 of N_1 (or on the washout parameter $K = \frac{\Gamma_1}{H_1}$), while the BE for the lepton asymmetry also depends on the asymmetry parameter ϵ. Solutions of these equations can be found in Ref. [19]. In the presence of multiple scalar fields (as described in Sec. II), the above BEs for leptogenesis have to be modified. The case with a single additional scalar field can be found in Ref. [10]. For simplicity, we consider explicitly the simplest two-scalar-field scenario. Modifications to the BEs arise from the correction to the Hubble parameter (as derived in Sec. II). With the assumption of $g_S \sim g_E$ for large T, the total radiation density can be extracted from Eqs. (16)–(18),

$$\rho_{\rm tot}(T) = \rho_{\rm rad}(T) + \sum_i^2 \rho_i(T) = \rho_{\rm rad}(T)\left\{1 + \left(\frac{T}{T_r}\right)^{n_1}\left[1 + \left(\frac{T}{T_2}\right)^{(n_2-n_1)}\right]\right\}, \tag{29}$$

where $T \ge T_2$ corresponds to the epoch of ϕ_2 scalar domination, $T_r \le T \le T_2$ represents that of ϕ_1-dominated expansion, while for $T \le T_r$ ($T_r = T_1$) the Universe is fully dominated by radiation. The modified Hubble parameter is thus

$$H_{\rm new} = H\left\{1 + \left(\frac{T}{T_r}\right)^{n_1}\left[1 + \left(\frac{T}{T_2}\right)^{(n_2-n_1)}\right]\right\}^{1/2}, \tag{30}$$

and it gives rise to the following modified BEs:

$$\frac{dY_{N_1}}{dz} = -z\frac{\Gamma_1}{H_1}\frac{1}{\mathcal{J}}\frac{\mathcal{K}_1(z)}{\mathcal{K}_2(z)}(Y_{N_1} - Y_{N_1}^{EQ}), \tag{31}$$

$$\frac{dY_L}{dz} = -\frac{\Gamma_1}{H_1}\frac{1}{\mathcal{J}}\left(\epsilon z\frac{\mathcal{K}_1(z)}{\mathcal{K}_2(z)}(Y_{N_1}^{EQ} - Y_{N_1}) + \frac{z^3\mathcal{K}_1(z)}{4}Y_L\right). \tag{32}$$

A convenient and useful way to write $\mathcal{J}$ is

$$\mathcal{J} = \left\{1 + \left(\frac{M_1}{T_r z}\right)^{n_1}\left[1 + \left(\frac{M_1}{T_r x z}\right)^{(n_2-n_1)}\right]\right\}^{1/2}, \tag{33}$$

with $x = \frac{T_2}{T_r}$. Looking into the modified BEs (31) and (32), it can be observed that, apart from the standard parameters ϵ and $K = \frac{\Gamma_1}{H_1}$, leptogenesis with two scalar fields depends on a set of four new parameters—$n_1, n_2($ or $n_2 - n_1), T_r/M_1$, and x (or T_2)—which naturally modify the abundance of lepton asymmetry Y_L as compared to that of standard leptogenesis. We numerically solve Eqs. (31) and (32), considering two possible sets of initial conditions. The first, A, corresponds to the case where the abundance of the RHN N_1 is the same as that at the equilibrium, $Y_{N_1}^{\rm in} = Y_{N_1}^{\rm eq}$. The second set, B, corresponds to a scenario in which the initial abundance of RHNs vanishes, i.e., $Y_{N_1}^{\rm in} = 0$. In both cases, we assume that lepton asymmetry is absent before the decay of N_1, $Y_L^{\rm in} = 0$. In the next two subsections we discuss in detail the solutions for the quantities involved in the modified BEs. Lepton asymmetry is partially converted into baryon asymmetry by sphalerons [19],

$$Y_B = \frac{8n_f + 4n_H}{22n_f + 13n_H} Y_L. \tag{34}$$

Note that $Y_B = \frac{28}{79} Y_L$ (for $n_H = 1$, $n_f = 3$), consistent with the observed baryon asymmetry of the Universe $Y_B = (8.24 - 9.38) \times 10^{-11}$ [25].

A. Case $Y_{N_1}^{\rm in} = Y_{N_1}^{\rm eq}$

In the left panel of Fig. 1, we show how the lepton asymmetry Y_L evolves as the Universe expands with z, considering the modified Hubble parameter of Eq. (30) for different n_1 but fixed $n_2 - n_1 = 1$ values. For the purpose of illustration, other relevant parameters are kept fixed. In particular, $\epsilon = 10^{-5}$ ($M_1 = 10^{11}$ GeV), $K = \frac{\Gamma_1}{H_1} = 600$, $T_r = 10^{-3} M_1$, and $T_2 = 5T_r$. We observe a relevant increase of Y_L as n_1 increases, which is expected because a higher n_1 corresponds to a faster expansion. Moreover, the increase of n_1 also dilutes in a considerable way the washout effect, as manifested by the lowering of the inverse decay to N_1.

In order to study the net effect of the presence of the second scalar, we consider a different $n_2 - n_1 = 2$ in the right panel of Fig. 1, keeping the same set of values for the remaining parameters as in the left panel. Comparing the two plots, it is quite clear that the second scalar field gives rise to an enhancement of the asymmetry Y_L accompanied by a clear lowering of the washout effect. For high values of n_1, however, the second scalar is less important because the influence of ϕ_1 is already very efficient, as demonstrated by the $n_1 = 3$ case where the fast expansion and the increase of Y_L lead to a negligible washout of the asymmetry. However, it is worth analyzing the dependence on the other involved parameters. For instance, the ratio between the temperatures separating the successive epochs of scalar domination is very important. To this aim, it is useful to plot the dependence of lepton asymmetry on the ratio of the two relevant temperatures: T_2 and $T_r = T_1$. The results are shown in Fig. 2 in the range $2 \leq T_2/T_r \leq 100$, for the two different values of $T_r = 10^{-2} M_1$ and $T_r = 10^{-3} M_1$, keeping the ϵ and K values as in Fig. 1. In the left panel, the curves correspond to different values of n_1 and $T_r = 10^{-2} M_1$, with solid lines corresponding to $n_2 - n_1 = 1$ and dashed lines to $n_2 - n_1 = 2$. The same plot with $T_r = 10^{-3} M_1$ is shown in the right panel. It happens that in the left-panel case the second scalar influences Y_L only if $T_2 \leq 10T_r$, increasingly proportionally to the difference $n_2 - n_1$and independently on the value of n_1. Notice that only for $n_1 = 3$ is it possible to get the required baryon abundance of the Universe by leptogenesis (black bar). The behavior changes drastically when $T_r = 10^{-3} M_1$, as shown in the right panel of Fig. 2. Indeed, the decrease of the ratio T_r/M_1 leads to a longer ϕ_1-dominance and naturally delays the beginning of the radiation era. Thus, it helps to move away the abundance of N_1 particles from the equilibrium, generating lepton asymmetry. It can be easily noticed that the enhancement of Y_L indeed satisfies baryon asymmetry already for

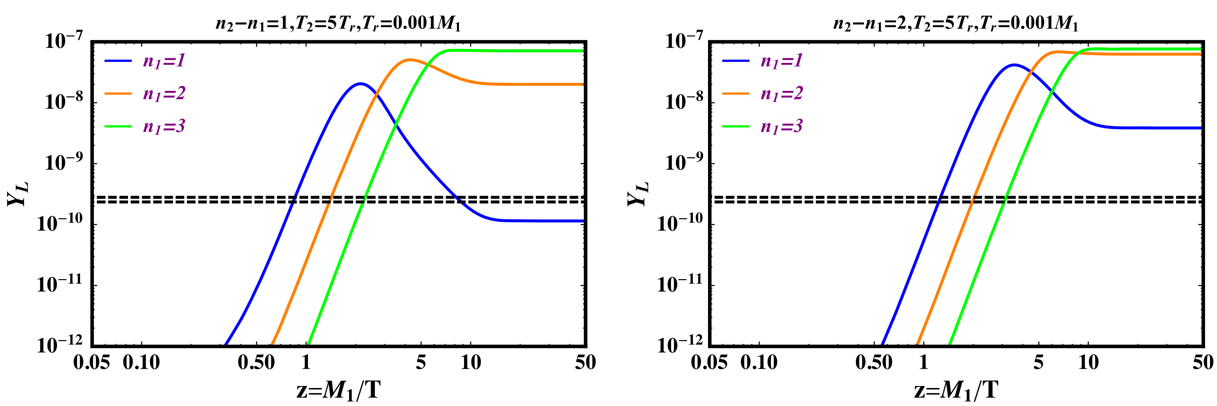

FIG. 1. Evolution of Y_L versus z for initial equilibrium RHN abundance, $T_2 = 5T_r$, and different n_1 values, with $n_2 - n_1 = 1$ (left panel) and $n_2 - n_1 = 2$ (right panel). The double black lines describe the baryogenesis threshold.

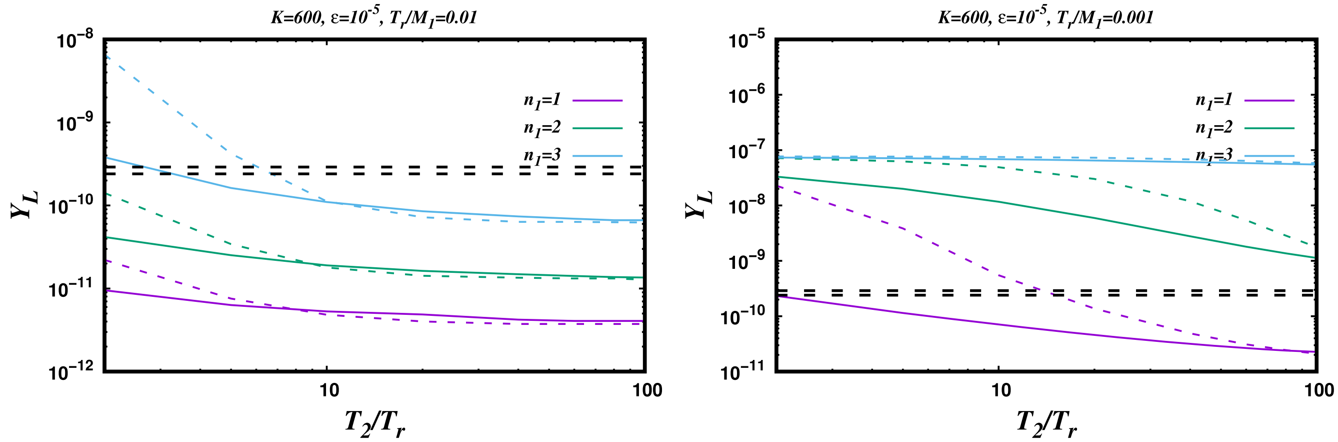

FIG. 2. Y_L versus T_2/T_r for $T_r/M_1 = 0.01$ (left panel) and $T_r/M_1 = 0.001$ (right panel), with different n_1. Solid (dashed) lines refer to $n_2 - n_1 = 1$ ($n_2 - n_1 = 2$). The double black lines describe the baryogenesis threshold.

$n_1 = 1$, and there is higher sensitivity to the difference $n_2 - n_1$, especially for large values of T_2/T_r, apart from the case when $n_1 = 3$ where, as in the previous analysis shown in Fig. 1, the washout is practically absent. Finally, it is worth observing that with the increase of T_2/T_r, the effects related to the presence of ϕ_2 become less and less important when the temperature decreases, becoming less prominent at the time of leptogenesis, as follows directly from Eq. (33). For example, for $T_r/M_1 = 0.01$, the possible choice $T_2/T_r = 100$ indicates that the influence of ϕ_2 on the Hubble parameter ceases to exist at $T = M_1$, while for $T_2/T_r = 10$ ϕ_2 remains active up to $T = 0.1\,M_1$, altering the abundance of Y_L. As it is clear from Eq. (33), the second-scalar effect dominates for $M_1/T_r \gg xz$, but becomes insignificant if $xz \geq 100$.

B. Case $Y_{N_1}^{\rm in} = 0$

In this section, we repeat the study of leptogenesis influenced by the presence of two scalars for a vanishing RHN initial abundance (the set of conditions B).

In Fig. 3, we show plots analogous to those in Fig. 1 using the same set of parameters: ϵ, M_1, T_r, T_2, K, and n_i. In this scenario, the initially produced N_1 is then partially compensated by the inverse decay, resulting in an oscillation of negative lepton asymmetry which later gives rise to the generation of a net positive lepton asymmetry. It should be noticed that for flavorless leptogenesis the BEs give rise to solutions with a single bounce in Y_L, while this is not the case in more general frameworks where additional bounces can occur, as shown in Ref. [26]. From the left panel of Fig. 3 it turns out that increasing the value of n_1 from 1 to 3 provides a reduced washout of asymmetry, resulting in an enhancement of the Y_L value. However, for $n_1 = 3$, the Y_L abundance value decreases significantly. This is due to the fact that a faster expansion also reduces the production of RHNs by inverse decay. Similar effects have already been observed in the presence of a single additional scalar field [10].

Moreover, this behavior becomes even more prominent when increasing $n_2 - n_1$, as depicted in the right panel of Fig. 3. Clearly, a faster expansion with respect to the $n_2 - n_1 = 1$ case tends to reduce the lepton asymmetry when starting from a situation where $Y_{N_1}^{\rm in} = 0$. Again, it is useful to study Y_L as a function of T_2/T_r. An analysis

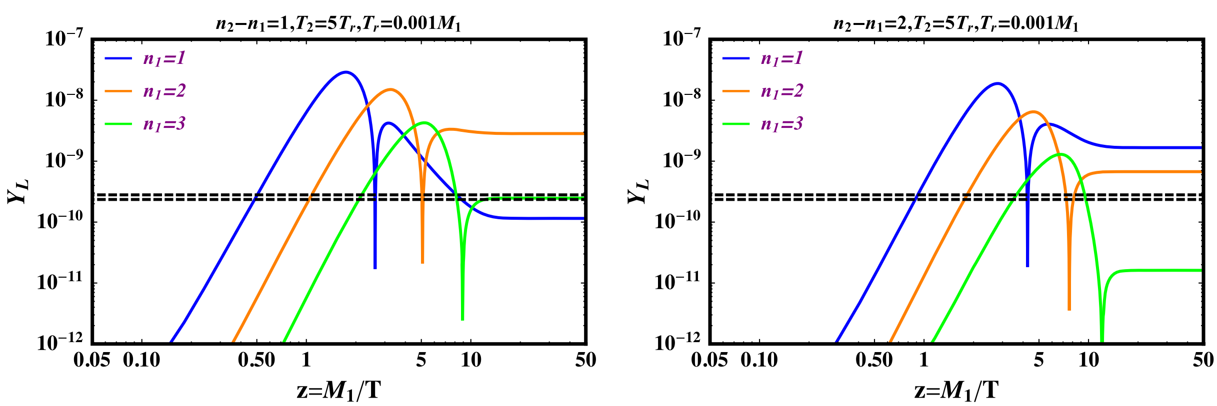

FIG. 3. Same as Fig. 1 for zero RHN abundance.

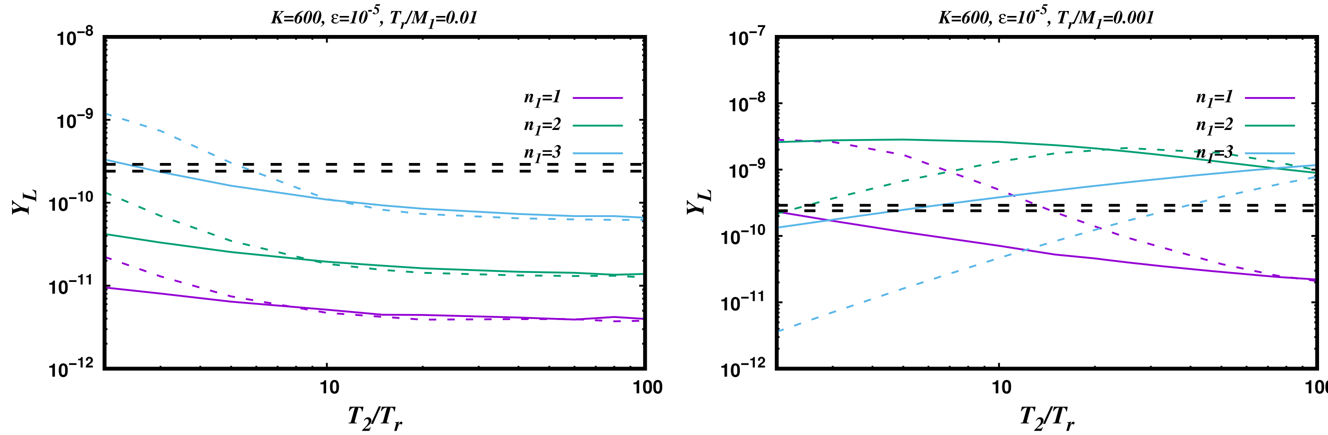

FIG. 4. Same as Fig. 2 with zero RHN initial abundance. The double black line describe the baryogenesis threshold.

similar to the one performed in the previous section leads to the plots in Fig. 4, related to the cases where $T_r/M_1 = 10^{-2}$ (left panel) and $T_r/M_1 = 10^{-3}$ (right panel). The parameters are kept fixed and are exactly the same as those in Fig. 2. For $T_r/M_1 = 10^{-2}$, the behavior of Y_L is very similar to that in the previous case in the left panel of Fig. 2 and also the analysis remains basically the same, although $Y^{\rm in}_{N_1} = 0$. In the case where $T_r/M_1 = 10^{-3}$, when compared with the right panel of Fig. 2, the quantitative results are quite different, but the qualitative behavior of Y_L with the ratio of T_2/T_r is again basically the same. The reduction of the final amount of asymmetry, as mentioned, is due to the relevance of the inverse decay which induces oscillations in the washout mechanism. In any case, the requested amount of baryon asymmetry can still be obtained for a large range of T_2/T_r values, at least when $T_r/M_1 = 10^{-3}$.

IV. NONSTANDARD HISTORY OF LEPTOGENESIS WITH THREE SCALAR FIELDS

It is quite difficult to solve the BEs for a generic number $k \geq 3$ of additional scalar fields. In order to guess the trend of the solutions, it is worth proceeding with the $k = 3$ example. Already in this case modifications of the BEs for leptogenesis are complicated, with an increased number of free parameters. The correction factor in this case reads

$$\mathcal{J} = \left\{1 + \left(\frac{M_1}{T_r z}\right)^{n_1}\left[1 + \left(\frac{M_1}{T_r xz}\right)^{(n_2-n_1)} \times\left(1 + \left(\frac{M_1}{T_r yz}\right)^{(n_3-n_2)}\right)\right]\right\}^{1/2}, \quad (35)$$

where $y = T_3/T_r$. Therefore, in the presence of three scalar fields, six new parameters ($n_i, i = 1, \ldots, 3$, T_r, x, and y) are necessary to introduce the modified Hubble rate. As described in Sec. II, in our setting of course $T_3 > T_2 > T_1 = T_r$, with successive ordered domination from ϕ_3 to radiation. Again, BEs for leptogenesis are solved for the two choices of the N_1 initial abundance already used in the two-scalar-field scenario.

A. Case $Y^{\rm in}_{N_1} = Y^{\rm eq}_{N_1}$

The Y_L abundance is shown in Fig. 5 for the initial conditions $Y^{\rm in}_{N_1} = Y^{\rm eq}_{N_1}$. The three curves in the left panel correspond to the different choices of $n_1 = 1$, 2, 3 and $T_3 = 10T_r$, $n_3 - n_2 = 1$. The other parameters (ϵ, M_1, K, T_2, and T_r) are kept fixed at the same values considered in Fig. 1. Again, a comparison between the case with two scalar fields shows that the washout effect is further reduced in the case where it is non-negligible, i.e., $n_1 = 1$. The behavior is even more significant when $n_2 - n_1 = 2$, where the washout is already reduced in the presence of two scalar fields. The dependence on the new parameters T_3 and $n_3 - n_2$ is also worth exploring, since it can change the behavior of the solutions. To this aim, we take $T_2 = 5T_r$ and $T_r = 10^{-3}\,M_1$, and solve the BEs for the four combinations of $n_2 - n_1$ and $n_3 - n_2$ equal to 1 or 2, while also varying T_3 to be $10T_r$, $50T_r$, or $100T_r$.

All of the resulting Y_L abundances are plotted in Fig. 6. In the upper-left panel, it can be observed that, with increasing T_3, the washout effect becomes prominent and the lepton asymmetry Y_L decreases. This is obvious because an increase in T_3 makes the third scalar insignificant. Indeed, for $T_3 = 100T_r$ the dominance of the third scalar ends at $T_3 = M_1$, well before the decay of N_1, without influencing leptogenesis. On the contrary, for $T_3 = 10T_r$ it remains effective until $T_3 = 0.1\,M_1$, the time of leptogenesis. A similar behavior can be observed in the other three panels, with different choices of $n_3 - n_2$ and $n_2 - n_1$. The third scalar field affects Y_L when $n_3 - n_2$ increases, inducing a smaller washout, as is evident from the comparison of the $n_3 - n_2 = 2$ and $n_3 - n_2 = 1$ cases. It is also clear that the influence of the third scalar depends on the influence of the second scalar. In the lower panels, it can be observed that with increasing $n_2 - n_1$ the washout effect is sensibly reduced, (almost) independently of the presence of the third scalar. In conclusion, one may say that

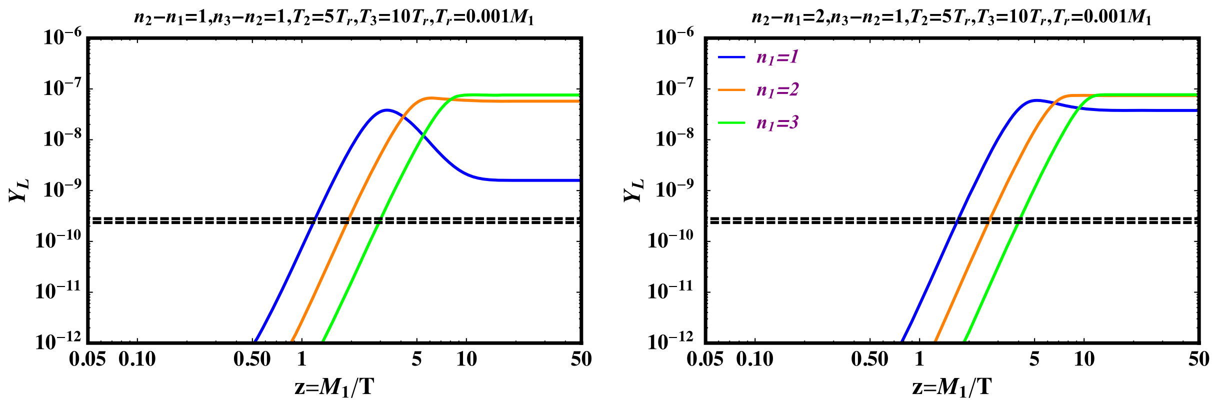

FIG. 5. Effect of three scalar fields on Y_L versus z plots for initial equilibrium RHN abundance and different n_1 values with $n_2 - n_1 = 1$ (left panel) and $n_2 - n_1 = 2$ (right panel), with $T_3 = 10T_r$ and $n_3 - n_2 = 1$. The double black lines describe the baryogenesis threshold.

an increase in both $n_3 - n_2$ and $n_2 - n_1$ results in a net decrease of the washout effect.

B. Case $Y_{N_1}^{\mathrm{in}} = 0$

Similarly to the previous discussion of leptogenesis in the presence of two additional scalar fields, in this section we analyze the possible effects due to a third scalar field in the case of a vanishing N_1 initial abundance. As before, in Fig. 7 we plot the values of Y_L against z for different n_1 and $n_2 - n_1 = 1, 2$. The remaining parameters are the same as those used in Fig. 5. There is a conspicuous amount of washout for the three reported values $n_1 = 1, 2, 3$ (left panel) at the initial stage, while in the second decay the washout is limited to the $n_1 = 1$ case.

Also, the Y_L value tends to decrease with increasing n_1, corresponding to the effect of less RHN production from

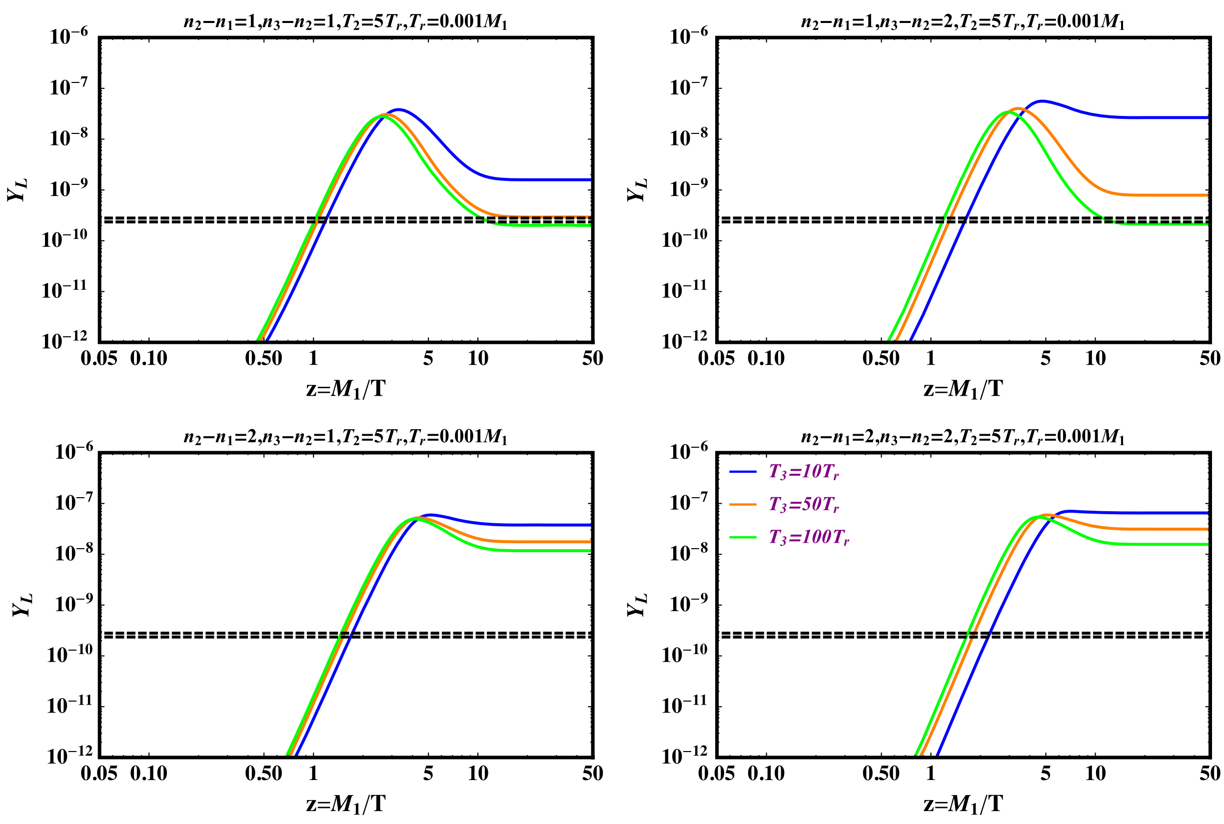

FIG. 6. Y_L versus z plots for $Y_{N_1}^{\mathrm{in}} = Y_{N_1}^{\mathrm{eq}}$ using various T_3/T_r values (10, 50, and 100) and different $n_3 - n_2$ and $n_2 - n_1$ combinations of values 1 and 2. The double black lines describe the baryogenesis threshold.

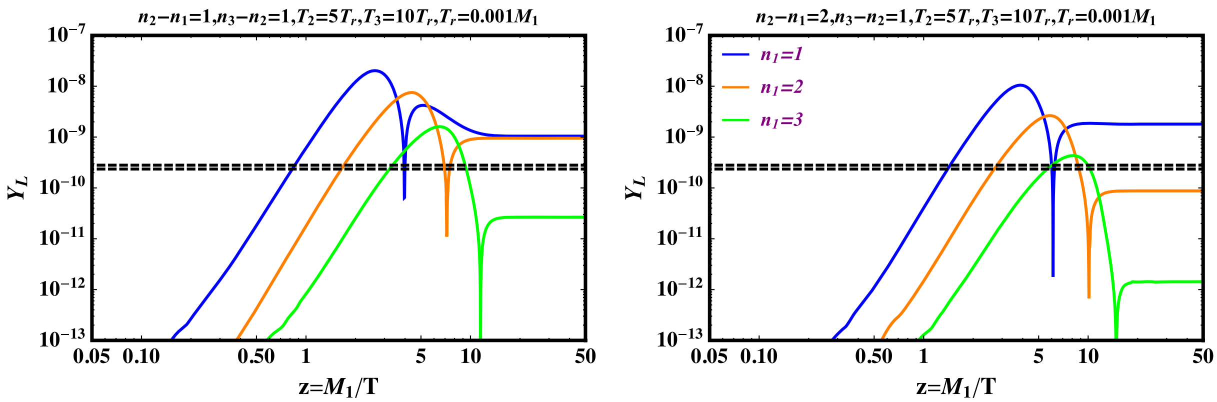

FIG. 7. Same as Fig. 5 for zero initial RHN abundance. The double black lines describe the baryogenesis threshold.

inverse decay due to the faster expansion of the Universe, as was already observed in the analogous scenario with two scalar fields. In the right panel, for $n_2 - n_1 = 2$, a similar behavior is slightly mitigated, with the $n_1 = 1$ case entering a regime of weak final washout. However, it should also be noticed that the value of Y_L is reduced as the net RHN production decreases due to a weaker inverse decay in a faster expansion. Again, it is also useful to extend the analysis related to Fig. 6 to the case of three scalar fields for a variable T_3/T_r and an initial vanishing N_1 abundance. An inspection of the four panels of Fig. 8 clearly demonstrates that increasing $n_2 - n_1$ or $n_3 - n_2$ results in an overall dilution of the washout of asymmetry. In spite of this, the transition from strong to weak washout does not ensure an enhancement of the Y_L value, which is also governed by the production of RHNs from the inverse decay. This fact can be easily seen, for instance, in the $T_3 = 10T_r$ plots (in blue) of Fig. 8. Initially, the lepton asymmetry enters a weak washout by changing $n_3 - n_2$ from 1 (upper-left panel) to 2 (upper-right panel), and Y_L

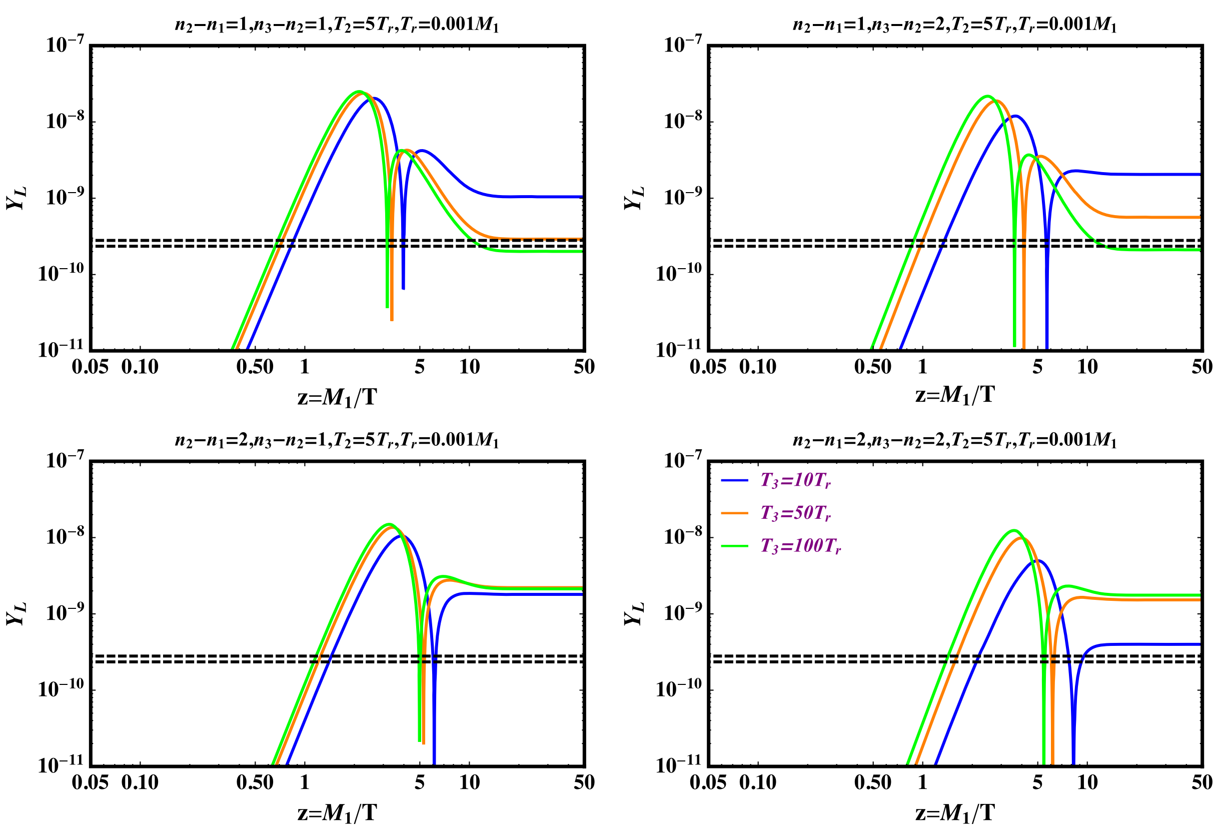

FIG. 8. Same as Fig. 6 for $Y_{N_1}^{\mathrm{in}} = 0$ with an identical color scheme for different choices of T_3. The double black lines describe the baryogenesis threshold.

increases. However, with a faster expansion ($n_2 - n_1 = 2$, lower-left panel) and even with a larger $n_3 - n_2 = 2$ (lower-right panel), Y_L decreases due to a compromised RHN production. Things are quite different for the $T_3 = 50T_r$ and $T_3 = 100T_r$ plots (yellow and green curves, respectively). The produced lepton asymmetry gradually enters a weak washout regime where it is enhanced (upper-right and lower-left panels), and finally saturates as the washout effect becomes negligible (lower-right panel). This behavior is quite different from the one shown in Fig. 6, and it is due to the combined effects of RHN production and the washout. As explained before, large values of T_3/T_r soften the influence of the third scalar field enhancing the washout, since the system stays longer far from an out-of-equilibrium phase (upper panels). These features disappear when the second scalar effect become stronger (lower panels). Finally, it should be stressed that the modifications to the BEs are basically linked to modifications of the effective Hubble rate, like that in Eq. (30) for the two-field case. It is thus natural to infer that our results are applicable to many other types of unflavored leptogenesis scenarios and are almost model independent.

V. DISCUSSION AND CONCLUSIONS

It is notoriously difficult to probe the dynamics of the early Universe in the epoch between cosmic inflation and the onset of BBN, whose predictions of primordial abundances of light elements are in very good agreement with measurements and represent one of the biggest successes of modern cosmology. The post-inflationary evolution is thus highly unconstrained, having only to be compatible with BBN. In particular, all of the cosmic relics that contribute to defining the ΛCDM cosmological model—like dark matter, dark energy, baryon abundances, radiation composition, and so on—crucially depend on the history around that time. Hence, the expansion rate can be drastically different compared to the standard cosmology in models where additional ingredients from fundamental (quantum or modified) gravity theories are present. For instance, four-dimensional (super)string models equipped with D-branes typically contain additional scalar species related to the positions of the branes in the transverse internal directions, which in nonequilibrium configurations could dominate the expansion rate before the radiation-dominated phase. It is plausible that these scalars are active during various processes in the Universe such as post-reheating, baryon asymmetry, leptogenesis, dark matter freeze-out or freeze-in, etc., and thus can significantly modify the thermal evolution of the Universe. In this paper, we addressed the effects of the presence of multiple additional (sterile) scalar fields with a faster-than-radiation dilution law in the post-reheating epoch that, if active at the scale of thermal leptogenesis ($T \sim 10^{12}$ GeV), can cause significant changes in the baryon asymmetry (via leptogenesis) of the Universe. In what follows, we briefly summarize our findings from the study of modified leptogenesis. The BEs describe the dynamics of the decay of the lightest RHN N_1, together with the evolution of the abundance of lepton asymmetry Y_L. In the presence of the k additional scalar fields defined in Sec. II, the standard BEs are modified basically by the introduction of an "effective" Hubble rate, $H_{\rm new}(T) = H(T)\mathcal{J}(T)$, where $\mathcal{J}$ is defined in Eq. (17). It depends on the exponents n_i, the "separating temperatures" T_i, and the effective degrees of freedom active at the corresponding epochs. Another important ingredient is represented by the initial conditions. We considered the two cases of $Y^{\rm in}_{N_1} = Y^{\rm eq}_{N_1}$ (condition set A), where the initial abundance of the RHN N_1 coincides with the abundance at equilibrium, and $Y^{\rm in}_{N_1} = 0$ (condition set B), with a vanishing initial abundance of N_1. The initial asymmetry $Y^{\rm in}_L$ was always taken to be vanishing. The main general results that can be extracted by numerical solutions of the BEs are the following:

(1) Typically, as n_i increases, Y_L increases while the washout decreases (see Figs. 1, 3, 5, and 7). This is due to the fact that the faster the expansion, the greater the departure from thermal equilibrium. As a consequence, the lesser inverse decay favours an enhancement of Y_L and a suppression of the washout.

(2) The relevance of ϕ_{i+1} with respect to ϕ_i depends on the difference $n_{i+1} - n_i$. It clearly grows if $n_{i+1} - n_i$ increases, but n_i must not be too high; otherwise, the dominance of ϕ_{i+1} enters too early, in an epoch where the RHN N_1 has not been produced in a sufficient quantity (see Figs. 2, 4, 6, and 8). In other words, if ϕ_i already absorbs the whole washout, the ϕ_{i+1} action ceases to be significant.

(3) In the evaluation of the ϕ_i contribution to leptogenesis, T_i is of course a fundamental parameter, since the field ϕ_i is active only if $T_i < M_1$. Moreover, if the ratio T_{i+1}/T_i decreases, the ϕ_{i+1}-domination epoch is longer and Y_L becomes bigger. All of the temperatures also have to be related to M_1 and $T_1 = T_r$.

(4) With the $Y^{\rm in}_{N_1} = Y^{\rm eq}_{N_1}$ initial conditions, the production of asymmetry Y_L is typically monotonic and after a washout the value of Y_L saturates at a certain value. To evaluate whether leptogenesis is efficient enough to generate the requested amount of baryon asymmetry, one has to analyze the balance between the values of the dilution exponents n_i and the ratios of the temperatures T_i to the radiation temperature T_r (see Figs. 1, 2, 5, and 6).

(5) With the $Y^{\rm in}_{N_1} = 0$ initial conditions, there is an oscillation due to the strong initial washout, since the inverse decay of the produced RHN N_1 is large at the beginning and starts with a vanishing initial abundance. The saturation of Y_L at a certain value is thus slower and the amount of asymmetry Y_L can be

small. As in the previous case, in order to understand whether leptogenesis can generate baryogenesis, one has to evaluate the dependence of Y_L on the n_i and the temperatures T_i (see Figs. 3, 4, 7, and 8).

(6) However, it is quite clear that in general more scalar fields contribute to an increase in the value of the asymmetry Y_L and in the worst case become ineffective for the reasons mentioned above. However, with a vanishing initial N_1 abundance, due to a weaker inverse decay in a faster expansion, there is a reduction of the saturated Y_N value.

(7) We have studied in detail the case with two scalar fields, where it is indeed possible to satisfy the baryon asymmetry of the Universe within the range $0.001 \leq T_r/M_1 \leq 0.01$ for thermal leptogenesis with the chosen set of parameters $M_1 = 10^{11}$ GeV, $\epsilon = 10^{-5}$, and $K = 600$ (see Sec. III) for a large interval of T_2/T_r values (see Figs. 2 and 4).

(8) In the case of three scalar fields, which we also studied in detail, it is important to analyze the behavior of the system with initial conditions $Y^{\rm in}_{N_1} = 0$ in comparison with the $Y^{\rm in}_{N_1} = Y^{\rm eq}_{N_1}$ initial conditions. Again, as in the presence of two scalar fields, a decrease in the washout accompanied by a decrease in the Y_L values can be observed. Moreover, we found that leptogenesis can generate baryogenesis in the interval $10 \leq T_3/T_r \leq 100$ for different values of $n_2 - n_1$ and $n_3 - n_2$ (see Sec. IV and Figs. 6 and 8 for details).

It is important to notice that since the modifications in leptogenesis are obtained by changing the Hubble parameter into the effective one, we expect that our findings will be applicable to any other thermal leptogenesis models, independent of the choice of the seesaw mechanism. Therefore, one can actually obtain a different regime of consistent parameter space in model-dependent studies due to the influence of these scalar fields.

The scale of leptogenesis in the case of a typical type-I seesaw model discussed in the present work is very high and is out of reach for the ongoing experimental facilities because the RHN mass is above 10^9 GeV [19]. In general, one may only get indirect signals for leptogenesis via observations of neutrinoless double-beta decay [27], via CP violation in neutrino oscillations [28], from the structure of the mixing matrix [29], or from constraints relying on Higgs vacuum metastability in the early Universe [30,31], which tightly pin down very the parameter space of heavy neutrino physics [32].

Several mechanisms with a much lower leptogenesis scale exist where the RHN masses arise due to new physics around the TeV scale if two RHNs are nearly degenerate in mass, known as *resonant leptogenesis* [33], or via oscillations of GeV-scale right-handed neutrinos [34] or via Higgs decay [35] as well as a dark-matter-assisted scenario with one- to three-body decays [36] which allow these models to be probed at the ongoing experimental facilities. In such models, it is plausible to obtain successful leptogenesis via RHNs with mass $M_1 \sim 10$ TeV, assuming an initial thermal abundance for RHNs along with an near absence of washout. It is possible that the scalar fields discussed in the present work may remain active at low scales as well. Therefore, we expect results that are completely different from the ones occuring in such low-scale leptogenesis models once a different thermal expansion is invoked via scalars but remaining above the energy scale where the sphalerons are active to transfer the asymmetry to the baryon sector. Moreover, possible observations of primordial gravitational waves sourced by topological defects [37], colliding vacuum bubbles [38], primordial black holes [39], and cosmic microwave background radiation measurements [40] should represent additional and complementary tools to probe leptogenesis at high energy scales. However, it should be stressed that these kind of nonstandard effective scalar field models provide the same cosmological predictions of other mechanisms, leaving room for a degeneracy. In this respect, it would thus be interesting to understand if there can be experimental probes of the proposed scenario.

ACKNOWLEDGMENTS

A. D. B. acknowledges financial support from DST, India, under Grant number IFA20-PH250 (INSPIRE Faculty Award). This work is supported in part by the DyConn Grant of the University of Rome “Tor Vergata”.

[1] The first version of an early accelerated universe is due to Alexei Starobinsky: A. A. Starobinsky, A new type of isotropic cosmological models without singularity, Phys. Lett. **91B**, 99 (1980); The first model of inflation as solution of the Big Bang puzzles is due to Alan Guth and implemented a strong first order phase transition; A. H. Guth, The inflationary universe: A possible solution to the horizon and flatness problems, Phys. Rev. D **23**, 347 (1981); A. D. Linde, A new inflationary universe scenario: A possible solution of the horizon, flatness, homogeneity, isotropy and primordial monopole problems, Phys. Lett. **108B**, 389 (1982); A. Albrecht and P. J. Steinhardt, Cosmology

for Grand Unified Theories with Radiatively Induced Symmetry Breaking, Phys. Rev. Lett. **48**, 1220 (1982); S. W. Hawking and I. G. Moss, Supercooled phase transitions in the very early universe, Phys. Lett. **110B**, 35 (1982); A. D. Linde, Chaotic inflation, Phys. Lett. **129B**, 177 (1983); For complete reviews see: A. D. Linde, Particle physics and inflationary cosmology, Contemp. Concepts Phys. **5**, 1 (1990); A. D. Linde, Inflationary cosmology, Lect. Notes Phys. **738**, 1 (2008); K. A. Olive, Inflation, Phys. Rep. **190**, 307 (1990); D. Baumann, Inflation, arXiv:0907.5424; J. P. Uzan, Inflation in the standard cosmological model, C. R. Phys. **16**, 875 (2015).

[2] B. A. Bassett, S. Tsujikawa, and D. Wands, Inflation dynamics and reheating, Rev. Mod. Phys. **78**, 537 (2006); A. V. Frolov, Non-linear dynamics and primordial curvature perturbations from preheating, Classical Quantum Gravity **27**, 124006 (2010); R. Allahverdi, R. Brandenberger, F. Y. Cyr-Racine, and A. Mazumdar, Reheating in inflationary cosmology: Theory and applications, Annu. Rev. Nucl. Part. Sci. **60**, 27 (2010); M. A. Amin, M. P. Hertzberg, D. I. Kaiser, and J. Karouby, Nonperturbative dynamics of reheating after inflation: A review, Int. J. Mod. Phys. D **24**, 1530003 (2014); K. D. Lozanov, Lectures on reheating after inflation, arXiv:1907.04402.

[3] F. D'Eramo, N. Fernandez, and S. Profumo, When the universe expands too fast: Relentless dark matter, J. Cosmol. Astropart. Phys. 05 (2017) 012.

[4] F. D'Eramo, N. Fernandez, and S. Profumo, Dark matter freeze-in production in fast-expanding universes, J. Cosmol. Astropart. Phys. 02 (2018) 046.

[5] A. Biswas, D. Borah, and D. Nanda, keV neutrino dark matter in a fast expanding universe, Phys. Lett. B **786**, 364 (2018); N. Fernandez and S. Profumo, Comment on "keV neutrino dark matter in a fast expanding universe" by Biswas *et al.*, Phys. Lett. B **789**, 603 (2019).

[6] H. Iminniyaz, B. Salai, and G. Lv, Relic density of asymmetric dark matter in modified cosmological scenarios, Commun. Theor. Phys. **70**, 602 (2018).

[7] B. Barman and A. Ghoshal, Probing pre-BBN era with scale invariant FIMP, J. Cosmol. Astropart. Phys. 10 (2022) 082.

[8] A. Maharana and I. Zavala, Postinflationary scalar tensor cosmology and inflationary parameters, Phys. Rev. D **97**, 123518 (2018).

[9] A. Di Marco, G. Pradisi, and P. Cabella, Inflationary scale, reheating scale, and pre-BBN cosmology with scalar fields, Phys. Rev. D **98**, 123511 (2018); See also: A. Di Marco, G. De Gasperis, G. Pradisi, and P. Cabella, Inflationary gravitational waves and exotic pre Big Bang Nucleosynthesis cosmology, J. Phys. Conf. Ser. **1548**, 012010 (2020); for the dependency of the tensor-to-scalar ratio parameter *r* on the reheating properties.

[10] S. L. Chen, A. Dutta Banik, and Z. K. Liu, Leptogenesis in fast expanding Universe, J. Cosmol. Astropart. Phys. 03 (2020) 009.

[11] M. Chakraborty and S. Roy, Baryon asymmetry and lower bound on right handed neutrino mass in fast expanding Universe: An analytical approach, arXiv:2208.04046.

[12] D. Mahanta and D. Borah, TeV scale leptogenesis with dark matter in non-standard cosmology, J. Cosmol. Astropart. Phys. 04 (2020) 032; D. Mahanta and D. Borah, WIMPy leptogenesis in non-standard cosmologies, arXiv:2208.11295; Z. F. Chang, Z. X. Chen, J. S. Xu, and Z. L. Han, FIMP dark matter from leptogenesis in fast expanding universe, J. Cosmol. Astropart. Phys. 06 (2021) 006.

[13] F. D'Eramo and K. Schmitz, Imprint of a scalar era on the primordial spectrum of gravitational waves, Phys. Rev. Res. **1**, 013010 (2019); N. Bernal, A. Ghoshal, F. Hajkarim, and G. Lambiase, Primordial gravitational wave signals in modified cosmologies, J. Cosmol. Astropart. Phys. 11 (2020) 051; A. Ghoshal, L. Heurtier, and A. Paul, Signatures of non-thermal dark matter with kination and early matter domination: Gravitational waves versus laboratory searches, arXiv:2208.01670.

[14] T. Koivisto, D. Wills, and I. Zavala, Dark D-brane cosmology, J. Cosmol. Astropart. Phys. 06 (2014) 036.

[15] A. Sagnotti, Open strings and their symmetry groups, arXiv:hep-th/0208020; G. Pradisi and A. Sagnotti, Open string orbifolds, Phys. Lett. B **216**, 59 (1989); P. Horava, Strings on world sheet orbifolds, Nucl. Phys. **B327**, 461 (1989); P. Horava, Background duality of open string models, Phys. Lett. B **231**, 251 (1989); M. Bianchi and A. Sagnotti, On the systematics of open string theories, Phys. Lett. B **247**, 517 (1990); M. Bianchi, G. Pradisi, and A. Sagnotti, Toroidal compactification and symmetry breaking in open string theories, Nucl. Phys. **B376**, 365 (1992); For reviews see: E. Dudas, Theory and phenomenology of type I strings and M theory, Classical Quantum Gravity **17**, R41 (2000); C. Angelantonj and A. Sagnotti, Open strings, Phys. Rep. **371**, 1 (2002); **376**, 407(E) (2003); R. Blumenhagen, B. Kors, D. Lust, and S. Stieberger, Four-dimensional string compactifications with D-branes, orientifolds and fluxes, Phys. Rep. **445**, 1 (2007).

[16] M. Fukugita and T. Yanagida, Baryogenesis without grand unification, Phys. Lett. B **174B**, 45 (1986); M. A. Luty, Baryogenesis via leptogenesis, Phys. Rev. D **45**, 455 (1992); M. Plumacher, Baryogenesis and lepton number violation, Z. Phys. C **74**, 549 (1997); R. Barbieri, P. Creminelli, A. Strumia, and N. Tetradis, Baryogenesis through leptogenesis, Nucl. Phys. **B575**, 61 (2000); G. F. Giudice, A. Notari, M. Raidal, A. Riotto, and A. Strumia, Towards a complete theory of thermal leptogenesis in the SM and MSSM, Nucl. Phys. **B685**, 89 (2004); W. Buchmuller, P. Di Bari, and M. Plumacher, Cosmic microwave background, matter—antimatter asymmetry and neutrino masses, Nucl. Phys. **B643**, 367 (2002); **793**, 362 (2008); A. Anisimov, S. Blanchet, and P. Di Bari, Viability of dirac phase leptogenesis, J. Cosmol. Astropart. Phys. 04 (2008) 033; H. Davoudiasl and Y. Zhang, Baryon number violation via majorana neutrinos in the early universe, at the LHC, and deep underground, Phys. Rev. D **92**, 016005 (2015); P. Hernández, M. Kekic, J. López-Pavón, J. Racker, and J. Salvado, Testable baryogenesis in Seesaw models, J. High Energy Phys. 08 (2016) 157; M. J. Dolan, T. P. Dutka, and R. R. Volkas, Dirac-phase thermal leptogenesis in the extended Type-I Seesaw model, J. Cosmol. Astropart. Phys. 06 (2018) 012.

[17] R. N. Mohapatra and G. Senjanovic, Neutrino masses and mixings in gauge models with spontaneous parity violation, Phys. Rev. D **23**, 165 (1981); C. Wetterich, Neutrino masses and the scale of B-L violation, Nucl. Phys. **B187**, 343 (1981); J. Schechter and J. W. F. Valle, Neutrino decay and

spontaneous violation of lepton number, Phys. Rev. D **25**, 774 (1982); B. Brahmachari and R. N. Mohapatra, Unified explanation of the solar and atmospheric neutrino puzzles in a minimal supersymmetric SO(10) model, Phys. Rev. D **58**, 015001 (1998); G. D'Ambrosio, T. Hambye, A. Hektor, M. Raidal, and A. Rossi, Leptogenesis in the minimal supersymmetric triplet seesaw model, Phys. Lett. B **604**, 199 (2004); T. Hambye and G. Senjanovic, Consequences of triplet seesaw for leptogenesis, Phys. Lett. B **582**, 73 (2004); S. Antusch, Flavour-dependent type II leptogenesis, Phys. Rev. D **76**, 023512 (2007); T. Hambye, Leptogenesis: Beyond the minimal type I seesaw scenario, New J. Phys. **14**, 125014 (2012); D. Borah and M. K. Das, Neutrino masses and leptogenesis in Type I and Type II Seesaw models, Phys. Rev. D **90**, 015006 (2014); M. Chakraborty, M. K. Parida, and B. Sahoo, Triplet leptogenesis, Type-II Seesaw dominance, intrinsic dark matter, vacuum stability and proton decay in minimal SO(10) breakings, arXiv:1906.05601; R. Foot, H. Lew, X. G. He, and G. C. Joshi, Seesaw neutrino masses induced by a triplet of leptons, Z. Phys. C **44**, 441 (1989); S. L. Chen and X. G. He, Leptogenesis and LHC physics with Type III See-Saw, Int. J. Mod. Phys. Conf. Ser. **01**, 18 (2011); E. T. Franco, Type I + III seesaw mechanism and *CP* violation for leptogenesis, Phys. Rev. D **92**, 113010 (2015); S. Kashiwase and D. Suematsu, Baryon number asymmetry and dark matter in the neutrino mass model with an inert doublet, Phys. Rev. D **86**, 053001 (2012); S. Kashiwase and D. Suematsu, Leptogenesis and dark matter detection in a TeV scale neutrino mass model with inverted mass hierarchy, Eur. Phys. J. C **73**, 2484 (2013); T. Hugle, M. Platscher, and K. Schmitz, Low-scale leptogenesis in the scotogenic neutrino mass model, Phys. Rev. D **98**, 023020 (2018); D. Mahanta and D. Borah, Fermion dark matter with N_2 leptogenesis in minimal scotogenic model, J. Cosmol. Astropart. Phys. 11 (2019) 021; In supersymmetric models, the gravitino production impose important constraints on the reheating temperature that may cause problems for leptogenesis and baryogenesis, as first noticed in: M. Y. Khlopov and A. D. Linde, Is it easy to save the gravitino?, Phys. Lett. B **138**, 265 (1984).

[18] A. Zee, A theory of lepton number violation, neutrino majorana mass, and oscillation, Phys. Lett. **93B**, 389 (1980); **95**, 461(E) (1980); L. J. Hall and M. Suzuki, Explicit R-parity breaking in supersymmetric models, Nucl. Phys. **B231**, 419 (1984); A. Zee, Quantum numbers of majorana neutrino masses, Nucl. Phys. **B264**, 99 (1986); K. S. Babu, Model of "Calculable" majorana neutrino masses, Phys. Lett. B **203**, 132 (1988); **203**, 132 (1988); L. M. Krauss, S. Nasri, and M. Trodden, A model for neutrino masses and dark matter, Phys. Rev. D **67**, 085002 (2003); Y. Cai, J. D. Clarke, M. A. Schmidt, and R. R. Volkas, Testing radiative neutrino mass models at the LHC, J. High Energy Phys. 02 (2015) 161; K. S. Babu, P. S. B. Dev, S. Jana, and A. Thapa, Non-standard interactions in radiative neutrino mass models, J. High Energy Phys. 03 (2020) 006; For a review, see: Y. Cai, J. Herrero-García, M. A. Schmidt, A. Vicente, and R. R. Volkas, From the trees to the forest: A review of radiative neutrino mass models, Front. Phys. **5**, 63 (2017).

[19] W. Buchmuller, R. D. Peccei, and T. Yanagida, Leptogenesis as the origin of matter, Annu. Rev. Nucl. Part. Sci. **55**, 311 (2005); W. Buchmuller, P. Di Bari, and M. Plumacher, Leptogenesis for pedestrians, Ann. Phys. (Amsterdam) **315**, 305 (2005); S. Davidson, E. Nardi, and Y. Nir, Leptogenesis, Phys. Rep. **466**, 105 (2008); C. S. Fong, E. Nardi, and A. Riotto, Leptogenesis in the Universe, Adv. High Energy Phys. **2012**, 158303 (2012); S. Blanchet and P. Di Bari, The minimal scenario of leptogenesis, New J. Phys. **14**, 125012 (2012).

[20] D. Baumann and L. McAllister, *Inflation and String Theory* (Cambridge University Press, Cambridge, England, 2015), ISBN 978-1-107-08969-3, 978-1-316-23718-2.

[21] J. K. Erickson, D. H. Wesley, P. J. Steinhardt, and N. Turok, Kasner and mixmaster behavior in universes with equation of state $w > \tilde{1}$, Phys. Rev. D **69**, 063514 (2004).

[22] J. A. Casas and A. Ibarra, Oscillating neutrinos and $\mu \to e, \gamma$, Nucl. Phys. **B618**, 171 (2001).

[23] S. Davidson and A. Ibarra, A lower bound on the right-handed neutrino mass from leptogenesis, Phys. Lett. B **535**, 25 (2002).

[24] P. Gondolo and G. Gelmini, Cosmic abundances of stable particles: Improved analysis, Nucl. Phys. **B360**, 145 (1991).

[25] C. Patrignani *et al.* (Particle Data Group), Review of particle physics, Chin. Phys. C **40**, 100001 (2016).

[26] S. Pascoli, S. T. Petcov, and A. Riotto, Leptogenesis and low energy *CP* violation in neutrino physics, Nucl. Phys. **B774**, 1 (2007); A. Granelli, K. Moffat, and S. T. Petcov, Aspects of high scale leptogenesis with low-energy leptonic *CP* violation, J. High Energy Phys. 11 (2021) 149; G. J. Ding, S. F. King, J. N. Lu, and B. Y. Qu, Leptogenesis in SO(10) models with A_4 modular symmetry, J. High Energy Phys. 10 (2022) 071.

[27] S. Dell'Oro, S. Marcocci, M. Viel, and F. Vissani, Neutrinoless double beta decay: 2015 review, Adv. High Energy Phys. **2016**, 2162659 (2016).

[28] T. Endoh, S. Kaneko, S. K. Kang, T. Morozumi, and M. Tanimoto, *CP* Violation in Neutrino Oscillation and Leptogenesis, Phys. Rev. Lett. **89**, 231601 (2002).

[29] I. Esteban, M. C. Gonzalez-Garcia, M. Maltoni, I. Martinez-Soler, and T. Schwetz, Updated fit to three neutrino mixing: Exploring the accelerator-reactor complementarity, J. High Energy Phys. 01 (2017) 087.

[30] E. Bertuzzo, P. Di Bari, and L. Marzola, The problem of the initial conditions in flavoured leptogenesis and the Tauon N_2-dominated scenario, Nucl. Phys. **B849**, 521 (2011).

[31] S. Ipek, A. D. Plascencia, and J. Turner, Assessing perturbativity and vacuum stability in high-scale leptogenesis, J. High Energy Phys. 12 (2018) 111.

[32] D. Croon, N. Fernandez, D. McKeen, and G. White, Stability, reheating and leptogenesis, J. High Energy Phys. 06 (2019) 098.

[33] J. Liu and G. Segre, Reexamination of generation of baryon and lepton number asymmetries by heavy particle decay, Phys. Rev. D **48**, 4609 (1993); M. Flanz, E. A. Paschos, and U. Sarkar, Baryogenesis from a lepton asymmetric universe, Phys. Lett. B **345**, 248 (1995); **384**, 487(E) (1996); **382**, 447(E) (1996); M. Flanz, E. A. Paschos, U. Sarkar, and J. Weiss, Baryogenesis through mixing of heavy Majorana neutrinos, Phys. Lett. B **389**, 693 (1996); L. Covi, E. Roulet,

and F. Vissani, *CP* violating decays in leptogenesis scenarios, Phys. Lett. B **384**, 169 (1996); L. Covi and E. Roulet, Baryogenesis from mixed particle decays, Phys. Lett. B **399**, 113 (1997); A. Pilaftsis, Resonant *CP* violation induced by particle mixing in transition amplitudes, Nucl. Phys. **B504**, 61 (1997); A. Pilaftsis, *CP* violation and baryogenesis due to heavy Majorana neutrinos, Phys. Rev. D **56**, 5431 (1997); A. Pilaftsis and T. E. J. Underwood, Resonant leptogenesis, Nucl. Phys. **B692**, 303 (2004); W. Buchmuller and M. Plumacher, *CP* asymmetry in Majorana neutrino decays, Phys. Lett. B **431**, 354 (1998); A. Granelli, K. Moffat, and S. T. Petcov, Flavoured resonant leptogenesis at sub-TeV scales, Nucl. Phys. **B973**, 115597 (2021); P. S. Bhupal Dev, P. Millington, A. Pilaftsis, and D. Teresi, Flavour covariant transport equations: An application to resonant leptogenesis, Nucl. Phys. **B886**, 569 (2014); P. S. Bhupal Dev, P. Millington, A. Pilaftsis, and D. Teresi, Kadanoff–Baym approach to flavour mixing and oscillations in resonant leptogenesis, Nucl. Phys. **B891**, 128 (2015); S. Antusch, E. Cazzato, M. Drewes, O. Fischer, B. Garbrecht, D. Gueter, and J. Klaric, Probing leptogenesis at future colliders, J. High Energy Phys. 09 (2018) 124.

[34] E. K. Akhmedov, V. A. Rubakov, and A. Y. Smirnov, Baryogenesis via Neutrino Oscillations, Phys. Rev. Lett. **81**, 1359 (1998); T. Asaka and M. Shaposhnikov, The νMSM, dark matter and baryon asymmetry of the universe, Phys. Lett. B **620**, 17 (2005); J. Ghiglieri and M. Laine, GeV-scale hot sterile neutrino oscillations: A derivation of evolution equations, J. High Energy Phys. 05 (2017) 132; J. Ghiglieri and M. Laine, Precision study of GeV-scale resonant leptogenesis, J. High Energy Phys. 02 (2019) 014; J. Ghiglieri and M. Laine, Sterile neutrino dark matter via GeV-scale leptogenesis?, J. High Energy Phys. 07 (2019) 078; J. Ghiglieri and M. Laine, Sterile neutrino dark matter via coinciding resonances, J. Cosmol. Astropart. Phys. 07 (2020) 012.

[35] T. Hambye and D. Teresi, Higgs Doublet Decay as the Origin of the Baryon Asymmetry, Phys. Rev. Lett. **117**, 091801 (2016); T. Hambye and D. Teresi, Baryogenesis from L-violating Higgs-doublet decay in the density-matrix formalism, Phys. Rev. D **96**, 015031 (2017).

[36] A. Dasgupta, P. S. Bhupal Dev, S. K. Kang, and Y. Zhang, New mechanism for matter-antimatter asymmetry and connection with dark matter, Phys. Rev. D **102**, 055009 (2020); D. Borah, A. Dasgupta, and D. Mahanta, Dark sector assisted low scale leptogenesis from three body decay, Phys. Rev. D **105**, 015015 (2022).

[37] J. A. Dror, T. Hiramatsu, K. Kohri, H. Murayama, and G. White, Testing the Seesaw Mechanism and Leptogenesis with Gravitational Waves, Phys. Rev. Lett. **124**, 041804 (2020); B. Barman, D. Borah, A. Dasgupta, and A. Ghoshal, Probing high scale Dirac leptogenesis via gravitational waves from domain walls, Phys. Rev. D **106**, 015007 (2022); D. I. Dunsky, A. Ghoshal, H. Murayama, Y. Sakakihara, and G. White, Gravitational wave gastronomy, arXiv:2111.08750.

[38] P. Huang and K. P. Xie, Leptogenesis triggered by a first-order phase transition, J. High Energy Phys. 09 (2022) 052; A. Dasgupta, P. S. B. Dev, A. Ghoshal, and A. Mazumdar, Gravitational wave pathway to testable leptogenesis, arXiv:2206.07032; D. Borah, A. Dasgupta, and I. Saha, Leptogenesis and dark matter through relativistic bubble walls with observable gravitational waves, arXiv:2207.14226.

[39] N. Bhaumik, A. Ghoshal, and M. Lewicki, Doubly peaked induced stochastic gravitational wave background: Testing baryogenesis from primordial black holes, J. High Energy Phys. 07 (2022) 130.

[40] A. Ghoshal, D. Nanda, and A. K. Saha, CMB footprints of high scale non-thermal leptogenesis, arXiv:2210.14176.